

High Data Rate Simulation of Phase Shifters in Silicon-On-Insulator

*ChingEng PNG^{*1,2}, Minjie SUN², and SoonThor LIM^{1,2}*

¹Institute of High Performance Computing, #16-16 Connexis North, 1 Fusionopolis Way, 138632, Singapore

²Optic2Connect (O2C) Pte Ltd, 71 Ayer Rajah Crescent, Ayer Rajah Industrial Estate, 139951, Singapore

*Email: pngce@ihpc.a-star.edu.sg

Abstract

We report a methodology to study low-loss high-speed traveling-wave silicon Mach-Zehnder modulator with reduced series resistance. The methodology constitutes electrical parameters including, but not limited to, capacitance, conductance and transitioning times to model time response and effective complex refractive index from optical simulations of phase shifter arms and in turn model the phase change and resultant loss induced by each arm. Furthermore, our methodology incorporates microwave impedance and propagation loss under reverse bias characterized by S-parameter measurements. Our high-speed optical performances are simulated and benchmarked against experimental data based on eye-diagram measurements in on-off keying at 10Gbps, showing excellent agreement. This methodology provides best-in-class accuracy and are suitable when operating speeds are scaled to 50Gbps.

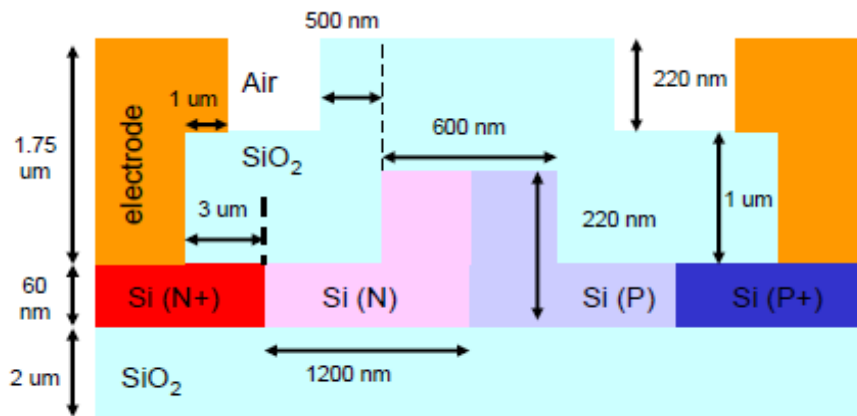
1. Introduction

High speed silicon optical modulators received significant research interest recently with multiple research groups and companies reporting multi-giga-bit-per-second (Gbps) performance [1]. A large number of such devices operate on the carrier depletion effect in a Mach-Zehnder Interferometer (MZI) setup [2-23]. A key factor to determine the performance of such devices, especially in GO/NO GO test is the high-speed eye diagram which reveals key information such as rise/fall times, extinction ratios, and jitter characteristics. However, in order to achieve realistic eye diagrams, actual fabricated device details such as topology and carrier induced losses must be encapsulated in the simulations including pseudo-random bit sequence (PRBS) generator, high speed oscilloscope etc. Optical device performance testing aided by computational tools will lead to cost and time savings and reduction of entry barrier into high speed telecommunication domain. Here we report a method to accurately analyze the optical signal output from Mach-Zehnder-Interferometer (MZI) configuration of modulators, allowing an unprecedented ability to predict electrical eye diagrams from electrical and optical simulation characteristics of individual modulators.

We evaluate the silicon-based MZI device by simulating the eye diagram based and its inherent electrical and subsequent optical modeling of individual silicon depletion modulator. This methodology directly takes into account the characteristics of a modulated optical beam, constituting electrical parameters such as capacitance, conductance, and transitioning times to model time response and to obtain effective complex refractive index from optical simulations of the phase shifter arms of the MZI. In turn this simulates the phase change and resultant loss induced by each arm. This methodology is suitable for interferometer-based optical devices and has been applied to silicon-based depletion modulators at 10-, 50-Gbps and demonstrated good agreement with experimental data. This development enables rapid design iterations with full accuracy and can be extended to other optical devices such as detectors and ring resonators.

2. Device Structure and Modulator Performance

In this paper, we evaluated high-speed optical eye diagrams for silicon modulators in MZI configuration as described in [2]. Figure-1 shows the schematic of the phase shifter. The optical modulation is achieved by arranging these phase shifter arms in MZI configuration, and each phase shifter consists of P-N junction and operated in depletion mode by applying a reverse bias. The effect of DC bias voltage on electrical behaviour of the modulator is calculated using physics-based device simulation. Physical models adopted here are found to be consistent with experimental data and implemented into our simulation models as per previous work [3-6]. Figure-2 shows the calculated capacitance and conductance for the different bias conditions. From these capacitance and conductance at 10 GHz frequency, the first time constant (τ_1) is calculated and compared against the time constant (τ_2) obtained from the rise/fall time of transient simulation (1V to 6V reverse bias) to determine effective time constant (τ). The step voltage is chosen as 1V to 6V, so as to be able to compare with the measured eye diagram reported in [2]. The time constant (τ) is used to model the step response of the input voltage change to the modulator arm.



From Figure-2, we can see the trend of capacitance (C) and conductance (G) with reverse bias voltage. As reverse bias voltage increases, conductance decreases. Increase in reverse bias voltage results in larger depletion region, which causes the conductance to decrease. However, the trend for capacitance is different in that first of all it increases and then starts to decrease as reverse bias voltage further increases. A sudden increase in capacitance for smaller reverse bias can be attributed to the appearance of depletion region at the beginning of reverse bias. However, when the reverse bias increases further the depletion region widens therein causing the capacitance to decrease. Additionally carrier concentration profiles obtained from electrical simulation are converted into complex refractive indices using an in-house developed code, based on Soref's equation [7], to accurately transfer electrical data into optical domain. To achieve greater accuracy in optical simulations, we input the map of the complex refractive index profile, as obtained from carrier refraction at the applied bias, across device cross-section. Figure-3 shows the bias dependent effective refractive index change (Δn_{eff}) and absorption coefficient (α). Refractive index and absorption coefficient are calculated from the real and imaginary part of complex effective index respectively. The applied bias is varied from 0V to -10V, i.e. reverse bias, which depletes the carriers from the junction of *p*-doped and *n*-doped regions. Δn_{eff} increases with the increasing reverse bias due to carrier depletion in the rib region. On the other hand, reduction in carriers decreases the carrier induced absorption of the light. Therefore, absorption coefficient decreases with an increase in the reverse bias voltage.

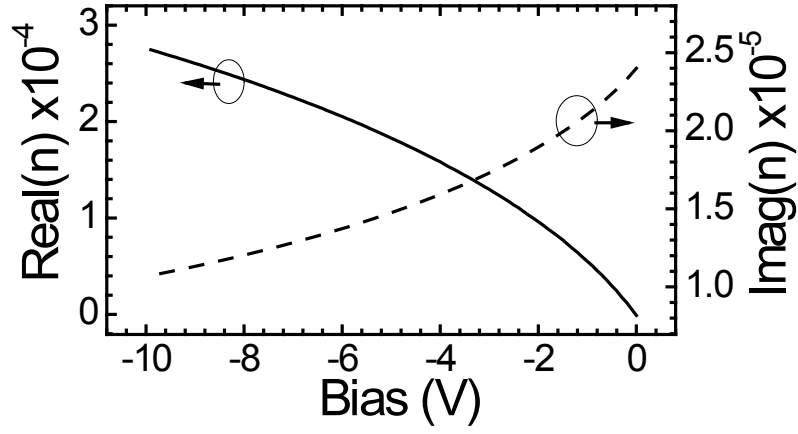


Figure 3. Bias dependent refractive index (real and imaginary n) change

3. Results of Optical Eye Diagrams

From these obtained time constants and effective indices, the eye diagram is calculated for the modulator figure-1. First of all a 10 Gbps pseudo random bit sequence (PRBS) is applied to the two arms of MZI. Each arm is 2 mm long with the DC bias, $V_{dc} = -3.75$ V, and rf signal, $V_{rf} = 5$ Vpp. Depending on the bit value input to the modulator arm consist of either $V_{dc} \pm V_{rf}/2$. Output optical beam is calculated from the interference of optical beams passing through two arms of MZI, as shown in figure-4, where calculated eye diagram (right in figure-4) is compared against the measured eye diagram (left in figure-4).

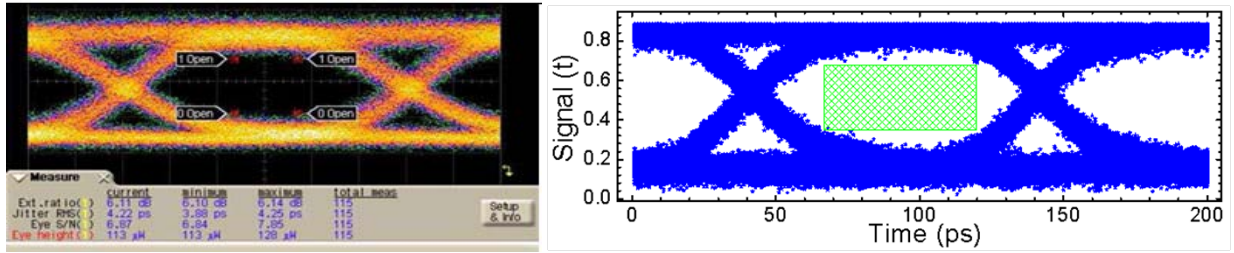


Figure 4. The simulated eye diagram using our method closely matches the experimental data. 10Gbps experimental optical eye diagram [2] (left), 10Gbps simulated optical eye diagram (right)

The calculated the eye diagram using the proposed method (using in-house developed software) shows excellent agreement with the measured eye diagram reported in [2]. Figure 4 shows the maximum intensity (I_{max}) and minimum intensity (I_{min}) of the optical pulse as 0.8 and 0.2 respectively, indicating an extinction ratio of 6 dB, calculated using $ER = 10 \log (I_{max}/I_{min})$, which is close to the reported ER of 6.1 dB in ref [2]. In figure-4 (right), there is a green box, which shows the noise margin available. The vertical noise margin signifies the modulator performance against the signal-to-noise ratio. The horizontal margin shows the modulator performance against the random jitter present in the electrical driving circuitry. Thus, this pioneered method allows us to replicate the measured results, give information about noise margin and extinction ratio, without the need for expensive equipment such as pattern generator, bit error rate tester (BERT) and high-speed oscilloscope.

4. Conclusions

This paper proposed a method to calculate high speed optical eye diagrams for silicon based optical modulators based on the MZI structure. The proposed method is applied to the depletion type of SOI modulators operating at 10 Gbps; the results of which show an excellent comparison with the measured eye diagrams. Thus, this development can help designers and researchers to perform design iterations with a high level of accuracy. The present developed code is tailored for generating eye diagrams in a MZI comprising two phase-shifter arms using carrier refraction mechanism. With further enhancement, this method can be extended to include other types of high speed optical devices such as ring resonators, and detectors with different length and driving bias conditions.

5. References

1. G. T. Reed, G. Mashanovich, F. Y. Gardes and D. J. Thomson, "Silicon optical modulators," *Nature Photon.* 4 (8), 518-526 (2010)
2. T. Y. Liow, K. W. Ang, Q. Fang, J. F. Song, Y. Z. Xiong, M. B. Yu, G. Q. Lo, D. M. Kwong, "Silicon Modulators and Germanium Photodetectors on SOI: Monolithic Integration, Compatibility, and Performance Optimization", *IEEE JSTQE* Vol. 16, No. 1 (2010)
3. C. E. Png, S. P. Chan, S. T. Lim, and G. T. Reed, "Optical Phase Modulators for MHz and GHz modulation in Silicon-On-Insulator (SOI)", *IEEE J. of Lightwave Tech.*, Vol 22, pp. 1573-1582 (2004)
4. M. Xin, A. J. Danner, C. E. Png, and S. T. Lim, "Cross waveguide resonator-based silicon electro-optic modulator with low power consumption", *J. of Opt. Soc. of America B (JOSA B)* 26 (11) 2176-2180 (2009)
5. F. Y. Gardes, G. T. Reed, N. G. Emerson, and C. E. Png, "A sub-micron depletion-type photonic modulator in silicon on insulator," *Opt. Express* 13 (2005)
6. M. Xin, C. E. Png, and A. J. Danner, "Breakdown delay-based depletion mode silicon modulator with photonic hybrid-lattice resonator", *Opt. Express*, Vol. 19, 5063-5076 (2011)
7. R. A. Soref, and B. R. Bennett, "Electro-optical effects in silicon," *IEEE J. Quantum Electron.* 23(1), 123–129 (1987)